Journal of Solid State Electrochemistry (2026) 30:2365–2371
https://doi.org/10.1007/s10008-025-06424-9

SHORT COMMUNICATION

# Bubble-guided chemical gardens growth in a confined space: straight tubes, worms and helices

D. Spanoudaki[1] · F. Brau[1] · A. De Wit[1]

Received: 30 May 2025 / Revised: 19 August 2025 / Accepted: 19 August 2025 / Published online: 27 August 2025
© The Author(s), under exclusive licence to Springer-Verlag GmbH Germany, part of Springer Nature 2025

## Abstract

In three-dimensional tanks, the bubble-guided growth of chemical garden tubes can be quite erratic. Here, we experimentally analyze the bubble-guided growth of such chemical gardens in quasi one-dimensional geometries using a co-flow microfluidic reactor. The confined environment tames the precipitation such that hollow straight tubes or thicker worm-like tubes can be obtained. In some regions of the parameter space spanned by the flow rate and the ratio of the bubble diameter to the inner width of the host capillary, an oscillatory motion of the bubble drives the growth of helices.

**Keywords** Chemical garden · Pattern · Helix · Precipitation · Flow

## Introduction

The far-from-equilibrium precipitation of chemical gardens has long drawn attention thanks to the beauty of the various erratic forms obtained when, typically, a seed of a metallic salt is poured into a three-dimensional (3D) beaker containing a silicate solution [1]. Meanwhile, their growth has been studied with various applications in mind, like the formation of biomimetic micro- and nanotubular forms [1–3], the development of new non-equilibrium materials synthesis paths [4], and even the investigation of life's emergence in terrestrial and extraterrestrial worlds [5–8].

Whereas properties of chemical gardens are nowadays well understood [1, 3], their controlled and reproducible growth is still a challenge. Understanding how to synthesize given chemical garden tubes with specific forms or compositions is a prerequisite to progress in their use for nonlinear materials synthesis.

Scientific approaches developed recently for the controlled growth of chemical gardens include: (1) the injection of a solution of one reactant into a 3D reservoir of the second reactant [9–11]; (2) the growth of pellets of controlled composition in a beaker of the other reactant, allowing the measurement of electrochemical potentials which are of particular interest for the understanding of life's emergence in marine vents [12]; (3) the two-dimensional (2D) growth by injection of one reactant into the other reactant initially filling the confined geometry of a Hele-Shaw cell (two glass plates separated by a thin gap) [13–18]; (4) precipitation in microfluidic devices [19, 20]; and (5) or formation of tubes in co-flow systems [21].

In some cases, the growth of chemical gardens can be controlled by an air bubble. Indeed, one of the most striking properties of classical chemical gardens grown in 3D beakers is that, sometimes, a bubble appears spontaneously and can guide the extension of a chemical garden branch when attached to its tip while rising in the 3D tank by buoyancy. This bubble-driven growth of chemical gardens was first reported by Hazlehurst [22], who described that air-capped chemical gardens grow in an erratic way. Bubble-guided chemical gardens have been studied in a more controlled way by using the injection method in a three-dimensional beaker [11, 23, 24]. With this approach, a gas bubble is attached to the tip of the growth zone of the tube where the inner solution is injected. As the inner fluid is injected, a precipitate tube grows, and the gas bubble remains connected to the top of the precipitate structure while more precipitate

This article is dedicated to Dimitra Sazou.

✉ A. De Wit
Anne.De.Wit@ulb.be

D. Spanoudaki
dimi.spanou@gmail.com

F. Brau
Fabian.Brau@ulb.be

[1] Nonlinear Physical Chemistry Unit, Université libre de Bruxelles, CP231, Bd du Triomphe, Brussels 1050, Belgium

is formed. Buoyancy forces cause the bubble to rise directly upwards, thus forcing the tubes to grow vertically [25]. Precipitate films over bubble surfaces and tube growth have also been observed via electrochemical processes in corrosion systems that are considered to belong to the chemobrionics field [1, 26, 27]. For instance, Stone and Goldstein [28], studying the electrochemical formation of iron tubes ("ferrotubes") on a steel cathode, also showed that the precipitate film forms over the bubble surface within seconds of its emergence from the tube. Self-organized structures on a zinc disc-electrode surface have also been shown to grow by a mechanism similar to that of chemical gardens [29], such that studies of new mechanisms of tube growth in chemical gardens can also benefit corrosion studies.

In parallel, other studies have tamed the growth of chemical gardens by reducing the spatial dimensions of the system. In quasi two-dimensional Hele-Shaw cells, a large variety of patterns like spirals, worms, and filaments are observed upon injection of one reactant solution into the bulk of the cell filled with the other reactant [13]. For high concentrations of both reactants, thin filaments grow with irregular turnarounds [13–18]. The reduced space allows to better quantify their growth dynamics [26, 30]. In quasi 1D reactors with injection, further control allows to grow controlled hollow tubes and extract new information about oscillatory dynamics [9, 21].

Here, we experimentally explore the growth of chemical garden tubes by combining bubble-guided growth and taming in a quasi one-dimensional co-flow system. We show that regular hollow tubes, worm-like patterns, as well as helices can be obtained depending on the injection flow rate and on the dimensionless bubble diameter. This paves the way to the use of flow conditions with controlled bubble guidance to master the choice of tube forms and their chemical properties in non-equilibrium conditions.

## Materials and methods

For the bubble-guided growth of chemical gardens, we use a custom-made reactor which consists of two concentric capillaries forming a co-flow geometry, as introduced in a previous study [21]. The capillaries of the microfluidic reactor are fluorinated ethylene propylene (FEP) chromatographic tubes (Vici Jour). The larger outer capillary initially containing silicate has an external diameter $d_{\text{out}}^{\text{Si}}$= 3.2 mm and an inner diameter $d_{\text{in}}^{\text{Si}}$ = 2.1 mm whereas the dimensions of the inner capillary through which the bubble followed by the cobalt chloride solution is injected has $d_{\text{out}}^{\text{Co}}$= 1.59 mm for the outer diameter and $d_{\text{in}}^{\text{Co}}$= 1.00 mm for the inner diameter. The two capillaries are connected with a Poly-Ether Ether Ketone (PEEK) junction positioned vertically on a plexiglass plate. The injection of the reactants is done using a neMESYS low-pressure pump syringe working with a BASE 120 controller.

The injected reactant is an aqueous 1.375 M cobalt chloride ($CoCl_2$) solution obtained by dissolving $CoCl_2.6H_2O$ (Sigma Aldrich) in distilled water, whereas the host reactant is a sodium silicate ($Na_2SiO_3$) solution, used as purchased from Sigma Aldrich, and with a chemical composition: $Na_2O$ = 10.6 %, $SiO_2$ = 26.5 %.

In all experiments presented here, the outer host solution is stagnant while the inner solution of $CoCl_2$ is injected with a constant flow rate $Q_{\text{Co}}$. Before injection starts, the inner $CoCl_2$ is initially separated from the silicate solution that fills the outer capillary by a given volume $V$ of air. When the air is completely pushed out of the inner capillary by the injected $CoCl_2$ solution, a bubble forms and precipitation starts on the bubble surface. The bubble is squeezed if its diameter $d = (6V/\pi)^{1/3}$ is smaller than the inner diameter of the outer tube $d_{\text{in}}^{\text{Si}}$. An important parameter of the problem, besides the flow rate $Q_{\text{Co}}$ is therefore the geometric parameter $\xi = d/d_{\text{in}}^{\text{Si}}$. If $\xi < 1$, the bubble has a diameter smaller than the width of the host outer tube and can thus rise in the gravity field by buoyancy without touching the walls, if initially well positioned at the center of the tube. On the contrary, if $\xi > 1$, the bubble is larger than the tube and will thus fill in the outer capillary while stretching vertically during its upward motion. Let us see how the presence of such a bubble of varying diameter can influence the growth of chemical garden precipitates in the co-flow reactor.

## Results and discussion

First, let us recall that a previous study has shown that, in the absence of any bubble, filaments grow in this co-flow set-up in an oscillatory way, forming precipitates with thin periodically spaced membranes on their surface [21]. Here, we analyze how the presence of a bubble can help to control this growth in a vertical set-up. If we introduce a bubble of a given volume $V$ at the tip of the inner tube, in front of the solution of $CoCl_2$ injected at a flow rate $Q_{\text{Co}}$, the bubble is pushed away and detaches from the tip of the tube. If the experiments are performed in tubes maintained in the horizontal direction, the growth of tubes systematically fails due to the buoyant tendency of the bubble to move in the upward direction. If the set-up is maintained vertically, regular precipitation tubes can be obtained in a large zone of parameters.

Upon injection of the inner reactant into the outer capillary, a reaction zone develops between the two fluids and the bubble, where a very thin precipitate membrane is formed. The bubble rises in the gravity field, templating the growth of the tube. Figure 1 shows examples of the various types of

**Fig. 1** Examples of precipitation patterns obtained in the co-flow system: **A** straight tube, **B** worm-tube, **C** helix, **D** unsuccessful experiment where the bubble (visible in the upper part inside the dashed rectangle) has taken a cylindrical shape, and **E** failed experiment where the bubble was trapped between the inner and outer FEP tubes. The precipitation occurred without the presence of a bubble. **F–I** Various forms of helices obtained. The scales of the photos are given by the outer diameter of the outer tube $d_{\text{out}}^{\text{Si}}$= 3.2 mm

precipitation patterns obtained. Three major types of regular tubes are obtained: straight tubes (Fig. 1A), larger tubes resembling worms (Fig. 1B), and spiraled tubes (Fig. 1C, F–I). In some cases, either no reaction occurs because the bubble prevents the mixing of the two reactants (Fig. 1D) or the bubble-guided precipitation fails simply because the bubble stays stuck between the two tubes (Fig. 1E). Note that the spiraled tubes are here driven by the oscillatory motion of the bubble and are thus different from precipitate helices obtained in horizontal flow systems [31].

## Parameter space

Figure 2 summarizes where the various precipitation patterns are observed in a parameter space spanned by the injection flow rate $Q_{Co}$ of the inner $CoCl_2$ solution and the bubble/tube aspect ratio $\xi$. For $\xi = 0.55$, straight precipitation tubes without any irregularities on their surface, such as the one shown in Fig. 1A, are obtained above a given flow rate. Their regularity is due to the fact that the bubble, having a smaller diameter than the tube, moves without any disturbance inside the outer tube, forming a thin, regular precipitation tube. Microscopy images taken after the experiment show that the precipitate is hollow and its inner and outer surfaces are smooth. If the flow rate is too small ($Q_{Co} = 10\ \mu L\ s^{-1}$ for example), the bubble-templated precipitation fails because the bubble stays attached to the inner tube and does not rise in the upward direction. In some cases, the bubble remains trapped between the inner and the outer FEP tubes and precipitation takes place without a bubble (Fig. 1E), leading to the formation of precipitates with membranes on their surface as seen previously in the same set-up in the absence of a bubble [21].

For larger $\xi$ (here $\xi = 0.93$ and 1.04), the bubble shape becomes cylindrical and fills totally the space between the cobalt chloride and silicate solutions upon entry into the outer tube. The dynamics then depend on the injection speed. For lower flow rates $Q_{Co} = 10$ or $40\ \mu L\ s^{-1}$, the bubble retains its cylindrical shape upon displacement, and acts like a piston, i.e., pushes gently the silicate solution out of the reactor without any contact with the $CoCl_2$ solution. This results in no precipitation as seen on Fig. 1D, where the upper part of the image shows that the red $CoCl_2$ solution is separated from the transparent silicate solution by a bubble of cylindrical shape (inside the dashed rectangle). For larger flow rates, we observe that the rising bubble starts to be squeezed and oscillates between the two opposite walls of the outer tube. This induces the formation of much larger worm-like tubes (Fig. 1B) invading the whole width of the outer tube. These tubes are hollow, as can be seen under the microscope (Fig. 3B).

For intermediate values of $\xi$ and lower values of $Q_{Co}$, new dynamics inducing helical precipitates are obtained. Specifically, for $Q_{Co} = 10$, 20 or 40 $\mu L\ s^{-1}$ and $\xi = 0.79$ (Fig. 2), we regularly obtain precipitate tubes that take a helix shape, as seen on Fig. 1C. For these values of parameters, the rising bubble oscillates between the two walls of the outer tube, templating the growth of the tube as a helical three-dimensional structure. Both right-handed and left-handed helices are obtained as the rising bubble has no preferable initial direction after leaving the inner tube (Fig. 4). Microscope images show that, after aging, the inner side of the helical precipitate takes a green color while the outer surface is rather white (Fig. 3A). This is related to the fact that cobalt-based precipitates can exhibit a wide variety of colors depending on their oxidation state, coordination sphere, and degree of hydration. In newly formed spiralled tubes, the fresh precipitate is green, which we attribute to the initial formation of cobalt(II) oxide [CoO] - silicate interfaces. On aging, however, the outer wall

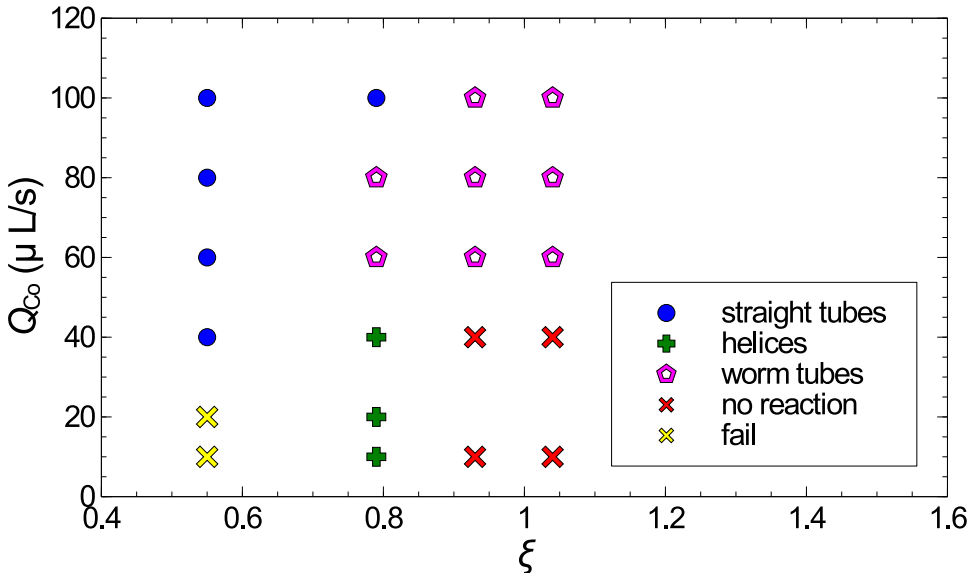


**Fig. 2** Summary of the observed type of pattern in the parameter space spanned by the injection flow rate $Q_{Co}$ of the inner solution of $CoCl_2$ and the bubble/tube aspect ratio $\xi$

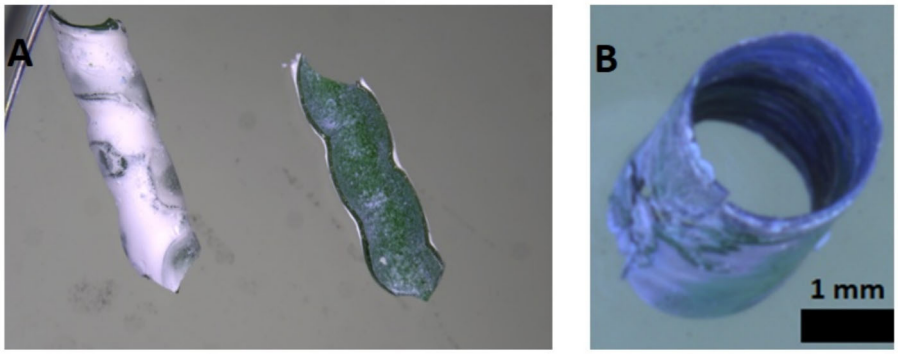


**Fig. 3** Microscope images of **A** the outer and inner surfaces of a helix after opening it in its middle and **B** a worm tube

of the tube comes in prolonged contact with the alkaline silicate solution and experiences further hydration and conversion of CoO to cobalt (II) hydroxide [$Co(OH)_2$], which is usually white in color. This explains why the outer surface of aged helices turns white while the inner part, which has lesser exposure to the silicate, retains the green coloring. These observations are consistent with those done on tubes obtained in the absence of bubbles [21], where precipitate tubes of different colors were recovered as a function of experimental conditions and extent of hydration or aging. In our case, the change in color reflects a progressive chemical evolution of the precipitate composition, from anhydrous or oxide-rich phases (green) to hydrated hydroxides (white).

A variety of helical precipitates has been obtained: (1) long helical precipitates (Fig. 1F), irregular twisted tubes (Fig. 1G), precipitates in which their initial and last part is a helix while a straight tube is created in between (Fig. 1H), helices with local flat surfaces giving twisted ribbons (Fig. 1I). For $Q_{Co} = 10\,\mu L\,s^{-1}$ and $\xi = 0.79$, almost 60 % of the experiments lead to no precipitation, while roughly 40 % feature the formation of helical precipitates, as shown in Fig. 1C. This suggests the proximity of a critical value of $Q_{Co}$ for $\xi = 0.79$ above which the rising bubble starts to oscillate, templating the helical precipitates.

Note that the phase space diagram of Fig. 2 gives a general indication of the values of parameters where typical patterns are obtained. In practice, the system is very sensitive to differences in initial conditions and to irregular motions of the bubble. Two main perturbations are regularly encountered: (1) the bubble can be trapped on the walls between the inner and outer FEP tube, resulting in precipitation patterns further downstream similar to those developing in absence of the bubble; (2) the bubble leaves the inner tube but slides without oscillating on the walls of the outer tube. Here again, precipitates similar to those previously studied without a bubble are obtained [21]. These two experimental problems cannot be avoided. Hence, multiple experiments need to be performed to obtain several regular helices.

## Tube widths

Figure 5 shows the average value of the width of the tube as a function of the injection flow rate for the straight tubes and the worm tubes. For $\xi = 0.55$, where straight tubes are obtained (Fig. 1A), the average width of the tube remains around the value of 1.6 mm independently of the $CoCl_2$ flow rate. The corresponding bubble diameter for $\xi = 0.55$ is 1.15 mm. The additional 0.45 mm is the thickness of the tube wall. For $\xi > 0.79$, where the worm tubes are observed (Fig. 1B), the average width is around 1.9 mm, meaning that the worms almost entirely invade the thickness of the reactor. In this case, the width of the precipitate tube is mainly controlled by the outer tube diameter.

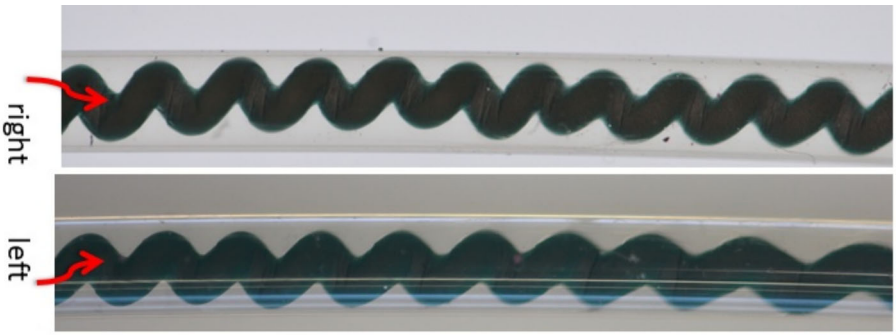


**Fig. 4** Example of left-handed and right-handed helices

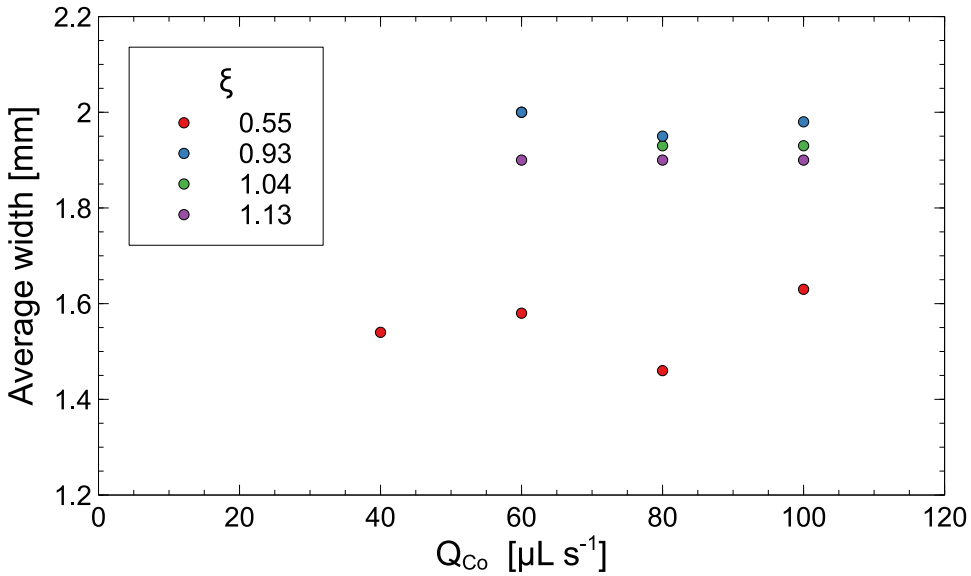


**Fig. 5** Average width of the tubes as a function of the injection flow rate $Q_{Co}$

## Conclusions

The bubble-guided growth of chemical garden tubes has been studied experimentally in a quasi-1-dimensional co-flow microfluidic device in which a solution of cobalt chloride is injected into a solution of silicate at a constant flow rate $Q_{Co}$. Various precipitation structures have been obtained when varying the injection flow rate and the bubble/inner tube aspect ratio $\xi$. If the $CoCl_2$ solution is injected at a sufficiently high velocity, straight tubes dominate at lower bubble size, while thicker worm tubes are obtained for larger bubbles. If the injection flow rate is too small, precipitation can either fail or produce some patchy, irregular precipitation structures. Nevertheless, for a given intermediate value of $\xi$ and low flow rates, very regular spiralled precipitation tubes are obtained when the bubble starts to have an oscillatory motion within the tube. The percentage of the right and the left-handed helices is roughly equal, meaning that there is no preference in the chirality of the precipitate. These results show that the use of a bubble to grow a chemical garden tube allows to control the width of the tube, switching from straight tubes of smaller diameters to larger worm tubes when the volume of the bubble is increased. Moreover, at lower injection speeds, helices can be obtained in some cases thanks to an oscillatory motion of the bubble in the confined geometry of the tube. This paves the way to analyze bubble-controlled growth of the tubes in quasi two-dimensional confined geometries, like in Hele-Shaw cells, where the additional degree of freedom could trigger new spatio-temporal dynamics.

**Acknowledgements** We acknowledge support from the M-ERA.NET Grant No. R. 50.12.17.F. A.D. further thanks Prodex and the FRS-FNRS PDR programme PHYLLO for financial support.

## Declarations

**Conflict of interest** The authors declare no competing interests.

## References

1. Barge LM, Cardoso SSS, Cartwright JHE, Cooper GJT, Cronin L, De Wit A, Doloboff IJ, Escribano B, Goldstein RE, Haudin F et al (2015) From chemical gardens to chemobrionics. Chem Rev 115(16):8652–8703
2. Nakouzi E, Steinbock O (2016) Self-organization in precipitation reactions far from the equilibrium. Sci Adv 2(8):1601144
3. Cardoso SSS, Cartwright JHE, Cejková J, Cronin L, De Wit A, Giannerini S, Horváth D, Rodrigues A, Russell MJ, Sainz-Díaz CI, Tóth A (2020) Chemobrionics: from self-assembled material architectures to the origin of life. Artif Life 26(3):315–326. https://doi.org/10.1162/artl_a_00323
4. Hughes EAB, Chipara M, Hall TJ, Williams RL, Grover LM (2020) Chemobrionic structures in tissue engineering: self-assembling calcium phosphate tubes as cellular scaffolds. Biomater Sci 8:812–822. https://doi.org/10.1039/C9BM01010F
5. Cartwright JHE, Russell MJ (2019) The origin of life: the submarine alkaline vent theory at 30. Interface Focus 9(6):20190104. https://doi.org/10.1098/rsfs.2019.0104
6. Hudson R, Graaf R, Strandoo Rodin M, Ohno A, Lane N, McGlynn SE, Yamada YMA, Nakamura R, Barge LM, Braun D, Sojo V (2020) $CO_2$ reduction driven by a pH gradient. Proc Natl Acad Sci USA 117(37):22873–22879. https://doi.org/10.1073/pnas.2002659117. https://arxiv.org/abs/https://www.pnas.org/content/117/37/22873.full.pdf
7. Mattia Bizzarri B, Botta L, Pérez-Valverde MI, Saladino R, Di Mauro E, García-Ruiz JM (2018) Silica metal oxide vesicles catalyze comprehensive prebiotic chemistry. Chem Eur J 24(32):8126–8132. https://doi.org/10.1002/chem.201706162. https://arxiv.org/abs/chemistry-europe.onlinelibrary.wiley.com/doi/pdf/10.1002/chem.201706162

8. Knoll P, Loron CC (2024) Effect of temperature on calcium-based chemical garden growth. ChemSystemsChem. 6:202400012. https://doi.org/10.1002/syst.202400012
9. Thouvenel-Romans S, Steinbock O (2003) Oscillatory growth of silica tubes in chemical gardens. J Am Chem Soc 125(14):4338–4341
10. Emmanuel M, Lantos E, Horváth D, Tóth A (2022) Formation and growth of lithium phosphate chemical gardens. Phys Chem Chem Phys 18:1731–1736. https://doi.org/10.1039/d1sm01808f
11. Zahorán R, Kumar P, Deák A, Lantos E, Horváth D, Tóth A (2023) From balloon to crystalline structure in the calcium phosphate flow-driven chemical garden. Langmuir 39:5078–5083
12. Glaab F, Kellermeier M, Kunz W, Morallon E, García-Ruiz JM (2012) Formation and evolution of chemical gradients and potential differences across self-assembling inorganic membranes. Angew Chem 51(18):4317–4321. https://doi.org/10.1002/anie.201107754
13. Haudin F, Cartwright JHE, Brau F, De Wit A (2014) Spiral precipitation patterns in confined chemical gardens. Proc Natl Acad Sci USA 111(49):17363–17367
14. Haudin F, Cartwright JHE, De Wit A (2015) Direct and reverse chemical garden patterns grown upon injection in confined geometries. J Phys Chem C 119(27):15067–15076
15. Haudin F, Brasiliense V, Cartwright JHE, Brau F, De Wit A (2015) Genericity of confined chemical garden patterns with regard to changes in the reactants. Phys Chem Chem Phys 17(19):12804–12811
16. Haudin F, De Wit A (2015) Patterns due to an interplay between viscous and precipitation-driven fingering. Phys Fluids 27:113101
17. Wagatsuma S, Higashi T, Sumino Y, Achiwa A (2017) Pattern of a confined chemical garden controlled by injection speed. Phys Rev E 95:52220
18. Wang Q, Bentley MR, Steinbock O (2020) Precipitate patterns in a Hele-Shaw cell with small sinusoidal height variations. J Phys Chem C 121:14120–14127
19. Batista BC, Steinbock O (2015) Growing inorganic membranes in microfluidic devices: chemical gardens reduced to linear walls. J Phys Chem C 119(48):27045–27052. https://doi.org/10.1021/acs.jpcc.5b08813
20. Nogueira JA, Batista BC, Cooper MA, Steinbock O (2023) Shape evolution of precipitate membranes in flow systems. J Phys Chem B 127:1471–1478. https://doi.org/10.1021/acs.jpcb.2c08433
21. Spanoudaki D, Brau F, De Wit A (2021) Oscillatory budding dynamics of a chemical garden within a co-flow of reactants. Phys Chem Chem Phys 23:1684–1693. https://doi.org/10.1039/D0CP05668E
22. Hazlehurst TH (1941) Structural precipitates: the silicate garden type. J Chem Educ 18(6):286. https://doi.org/10.1021/ed018p286
23. Thouvenel-Romans S, Pagano JJ, Steinbock O (2005) Bubble guidance of tubular growth in reaction-precipitation systems. Phys Chem Chem Phys 7(13):2610. https://doi.org/10.1039/b504407c
24. Pagano J, Bánsági T, Steinbock O (2008) Bubble-templated and flow-controlled synthesis of macroscopic silica tubes supporting zinc oxide nanostructures. Angew Chem Int Ed 47(51):9900–9903. https://doi.org/10.1002/anie.200803203
25. Rocha LAM, Cartwright JHE, Cardoso SSS (2022) Filament dynamics in vertical confined chemical gardens. Chaos 32:053107. https://doi.org/10.1063/5.0085834
26. Brau F, Haudin F, Thouvenel-Romans S, De Wit A, Steinbock O, Cardoso SSS, Cartwright JHE (2018) Filament dynamics in confined chemical gardens and in filiform corrosion. Phys Chem Chem Phys 20(2):784–793. https://doi.org/10.1039/c7cp06003c
27. Brau F, Thouvenel-Romans S, Steinbock O, Cardoso SSS, Cartwright JHE (2019) Filiform corrosion as a pressure-driven delamination process. Soft Matter 15:803–812. https://doi.org/10.1039/c8sm01928b
28. Stone DA, Goldstein RE (2004) Tubular precipitation and redox gradients on a bubbling template. Proc Natl Acad Sci USA 101(32):11537–11541. https://doi.org/10.1073/pnas.0404544101. https://arxiv.org/abs/www.pnas.org/content/101/32/11537.full.pdf
29. Spanoudaki D, Pavlidou E, Sazou D (2021) The growth of an electrochemical garden on a zinc electrode. ChemSystemsChem. 3:2000054. https://doi.org/10.1002/syst.202000054
30. Rocha LAM, Cartwright JHE, Cardoso SSS (2021) Filament dynamics in planar chemical gardens. Phys Chem Chem Phys 23:5222–5235. https://doi.org/10.1039/d0cp03674a
31. Knoll P, Gonzalez AV, McQueen ZC, Steinbock O (2019) Flow-induced precipitation in thin capillaries creates helices, lamellae, and tubes. Chem Eur J 25(61):13885–13889. https://doi.org/10.1002/chem.201903951


**Publisher's Note** Springer Nature remains neutral with regard to jurisdictional claims in published maps and institutional affiliations.